UNIVERSITI
MALAYSIA
PERLIS

Spin Coating Technique for the Synthesis of Hexagonal $Cd_xZn_{1-x}S$ Decorated Pure ZnO Nanorods Arrays

Araa Mebdir Holi [1]* and Asla Abdullah AL-Zahrani [2]

[1] *Department of Physics, College of Education, University of Al-Qadisiyah, Al-Diwaniyah, Al-Qadisiyah 58002, Iraq.*
[2] *Imam Abdulrahman bin Faisal University, Eastern Region, Dammam, Saudi Arabia .*

ABSTRACT

The thin films of $Cd_xZn_{1-x}S$, where x vary: 0.1, 0.3, 0.5, 0.7 and 0.9, have been synthesised by the spin coating technique using a ZnO nanorods/ITO glass as a substrate. The properties of structural, optical and photoelectrochemical have been studied. The pattern of X-ray diffraction of the optimum film $Cd_{0.9}Zn_{0.1}S$/ZnO NRs shows polycrystalline in nature and it has the favourite orientation laterally the (002) plane. The absorption edges of absorbance spectra of different x ($Cd_xZn_{1-x}S$) shifts towards lower wavelength with the increase in Zn concentration and these spectra were utilized in determining energy bandgap. Investigation indicated that the bandgap value increases with an increase in Zn content. The result disclosed an acceptable improvement in the photocurrent density of $Cd_{0.9}Zn_{0.1}S$/ZnO NRs (0.47 mA/cm^2) that was around 12 times greater than ZnO NRAs (0.04 mA/cm^2).

Keywords: $Cd_xZn_{1-x}S$, Spin-Coating Technique, Photoelectrochemical Cells, ZnO Nanorod Arrays.

1. INTRODUCTION

ZnO is one of the favourable optical-electronic materials due to its binding energy of exciton (60 meV) and large wide bandgap energy (3.37 eV). Many applications use ZnO thin films, for example, photoanodes for PEC cells [1-2], transparent electrodes [3], room temperature UV laser [4], solar cells [5], and, gas sensors [6]. Unfortunately, achieving visible light absorption from a single ZnO material is difficult to get. Many binary compounds such as CdS, Ag_2S, Bi_2S_3 have been used to deposit on the ZnO surface to enhance its ability to absorb visible light [7-9].

Numerous ternary CdZnS semiconductor films were prepared by chemical bath deposition (CBD) in order to study the absorption in the visible light [10]. The semiconductors of II–VI compound chalcogenide has gained the attention of a lot of scholars because of their applications in material science [11]. Composite materials can be produced when the elements of mercury, cadmium, and zinc combine with S, or Se and Te consist of II–VI compound semiconductors. Some remarkable photosensitive applications such as a photodetector, solar cell and laser used the II–VI semiconductors due to an adjustable bandgap [12].

In the latest years, theoretical and experimental works have been prepared to comprehend the vital properties of II–VI/semiconductors. One of the members of the II–VI group compound semiconductors is CdS, that has a suitable bandgap (2.40 eV). It is utilized widely as window material in photo-conducting cells. Additionally, this compound is also attractive for fabricating

---

Corresponding Author: araa.holi@qu.edu.iq

some devices such as heterojunction solar cells and nonlinear optical devices, and further optical-electronic devices in the spectrum wavelength between the blue (~360 nm) to ultraviolet (~490 nm) [13].

The $Cd_xZn_{1-x}S$ thin films are well-known, and they have some properties concerning of CdS and ZnS. Moreover, it possesses a large bandgap compared to CdS, making it more suitable as a window through solar cell fabrication [14] and photoelectrochemical cells [15]. Bandgap energy and CdZnS lattice constant values are adjusted since these parameters depend on Cd content to Zn ratio which is associated with the composition distinction of Cd and Zn in CdZnS. The thin films of CdZnS have formed the topic of significant attention in the various set of applications in the area of solid-state physics such as photoconductive devices and heterojunction photovoltaic solar cells [16,17].

Heterojunction between ternary compounds such as $CuGaSe_2$ or CdZnS, instead of a binary compound like CdS can enhance photoelectrochemical performance via the provision of the match in the electronic levels and lattice constants of both materials. Similarly, in heterojunction solar cells, the support of Zn in CdS improve the short circuit current and open-circuit voltage of the device simultaneously and exhibits higher conversion efficiency [18].

Many works have been archived on electrical, optical and structural properties of CdS and ZnS, which are all set by diverse methods such as chemical bath deposition [19,20], spray pyrolysis [21,22], vacuum evaporation [23,24], screen printing [25,26], and, sintering [27,28]. A number of researches available on the ternary CdZnS thin films synthesized via the vacuum evaporation method where an alloyed mix of CdS and ZnS were used in changing the compositions [29]. With respects to this, very little effort has been made to synthesize thin films of $Cd_xZn_{1-x}S$ by the spin coating method. In this work, the spin coating method was used with different ratios of x=[Cd]/[Cd]+[Zn] to deposit $Cd_xZn_{1-x}S$ films on ZnO NRs. Hence, the impact of Zn content in CdZnS on structural, optical and photoelectrochemical properties were thoroughly investigated.

2. MATERIAL AND METHODS

2.1 Experimental Methods

The ZnO nanorods decorated with $Cd_xZn_{1-x}S$ were prepared via various methods. Firstly, through a dip coating technique which was then followed by a hydrothermal growth treatment for depositing the pure ZnO nanorods on ITO glass (ZnO NRs/ITO). Then, the spin coating technique was used for depositing the $Cd_xZn_{1-x}S$ on ZnO NRs/ITO. Starting from the cleaning process of the substrates, all the methods were as the following: In order to ensure removal of impurities as well as to activate the surface, ITO glass substrates were sonicated in acetone, 2-propanol, and deionized water. The precursor solution was prepared by mixing 0.2 M diethanolamine with 0.2 M of zinc acetate dehydrate in ethanol solution for 30 minutes under the condition of 60°C and allowed for overnight ageing. Thereafter, the prepared precursor solution was coated onto ITO glass through the dip coating technique for 30 seconds and subsequently, the substrate was heated in an electric oven at 150°C for 5 minutes to remove the remaining solvent. The entire 3 covering films were deposited to certify a compact and identical spreading of ZnO seed layer. At that time, the layered substrates were heated at 350°C for the duration of 1 hour.

Hydrothermal growth handling was used to conserved samples that were covered with ZnO seed layer with thickness was around 140±20 nm to achieve the ZnO nanorods. A mix of 0.04 M zinc nitrate 6-hydrate and 0.04 M hexamethylenetetramine was prepared, and the annealed samples were later placed in the 20 ml beaker filled with the prepared mixture, trailed by

placing them into an electric oven for 4 hours at 150±5°C. Then, the heated samples were removed out from the beaker, rinsed with deionized water and allowed to dry.

The spin coating deposition of Cd_xZn_{1-x} S was maintained by different x=0.1, 0.3, 0.5, 0.7 and 0.9. The precursor aqueous solutions are 0.05 M Na_2S and 0.05 M $Cd(NO_3)_2$ throughout the study in order to investigate the effect of Zn^{2+} concentration on the growth of nano-film and that was calculated using the equation: x=[Cd]/[Cd]+[Zn]. The coated period was approximately 30 seconds at 2000 rpm. One spin coating cycle contained three steps: the substrate ZNR/ITO was spin coating 80 μl for the first reaction by aqueous precursors of $Cd(NO_3)_2$, subsequently $Zn(NO)_3$. Next, spin coating with an aqueous solution of Na_2S to react the S^- ions with adsorbed Cd^+ and Zn^+ ions on the substrate to form $Cd_xZn_{1-x}S$. This procedure was repeated four spin coating cycles for different x=0.1, 0.3, 0.5, 0.7 and 0.9.

2.2   Characterization

The field emission scanning electron microscopy (FESEM, JOEL JSM-7600F, Japan) equipped with INCA energy dispersive X-ray spectrometer (EDS) was utilized to inspect the surface morphology of the prepared pure ZnO, $Cd_{0.9}Zn_{0.1}S$ and elements analysis. The structure and phases of the pure ZnO and $Cd_{0.9}Zn_{0.1}S$ were analysed via X-ray diffractometry (Panalytical X'Pert Pro MPD diffractometer) by employing CuKα radiation (λ = 1.54 ˚A) at 40 mA and 40 kV. Similarly, absorbance spectra of the prepared sample were quantified using Lambda 20 Ultraviolet-visible spectrophotometer (Perkin Elmer Instruments). The photoelectrochemical measurement was conducted using linear sweep voltammetry (Autolab PGSTAT204/FRA32M module) in order to control the potential as well as recording the corresponding photocurrent at the scan rate of 20 mV s^{-1} in 0.1 M Na_2S mixture under illumination.

3.   RESULTS AND DISCUSSION

3.1 Optical Properties

The optical absorbance spectra recorded for the various x ratio [1:9; 3:7; 5:5, 7:3; 9:1] in the range of 350-600 nm as can be seen in Figure 1. This work only focused on the influence of Zn source concentration. From the inset Figure 1, it is clearly observed that the energy gap of the samples was affected by the concentration of Zn source. In Figure 2, the increasing x ratio from 0.1 to 0.9 is significant. The energy gap increased with decreased x ratio, then decreased with the more increasing of x ratio, which approves the merger of Zn ions into the CdS.
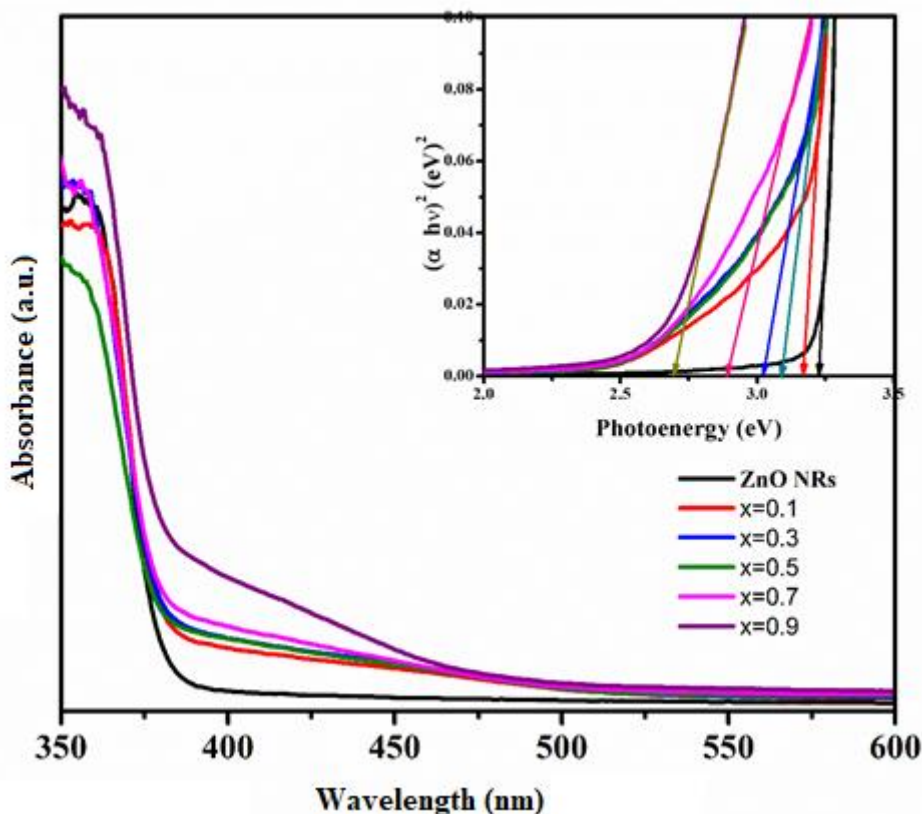
Figure 1. UV–vis spectra and bandgap energy curves (shown in insets of the figure) of (a) ZnO NRs/ITO, and Ag_2S NPs/ZnO NRs/ITO prepared at $Cd_xZn_{1-x}S$/ZnO NRs nanocomposites prepared at x.
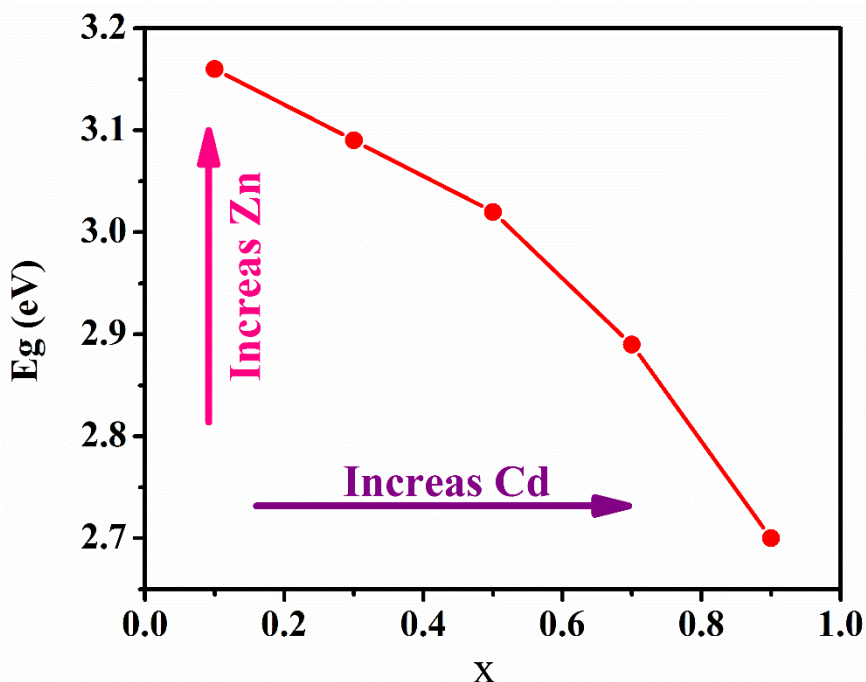

Figure 2. Bandgap energy values verses x=[Cd]/[Cd]+[Zn].

3.2 X-ray Diffraction Analysis

The crystal structure, as well as crystalline quality of ZnO/ITO and $Cd_{0.9}Zn_{0.1}S$/ZnO/ITO thin films, were examined using X-ray Diffraction (XRD) technique as shown in Figure 3. This was achieved with a diffraction angle ranging from 20° to 80°. The ZnO sample displayed hexagonal

phase as indicated by the scattering from (100), (002), (101), (102), (103), and (201) planes respectively which matched with 00-003-0888 ICSD reference card. The optimum sample $Cd_{0.9}Z_{0.1}S$ thin film was a hexagonal structure with preferred orientation of (100), (101), (220) and (203) at 26.62°, 30.19°, 47.1°, and 72.4° respectively.

The existence of overlapping peak (220) around 2θ value of 47.1° of ZnS, confirms the incorporation of Zn ions into the CdS lattice. The proposed results are in agreement with the previously published study by [30]. The crystallite size, D, of optimum sample $Cd_{0.9}Zn_{0.1}S$ was projected from the full width at half maximum (β) of the dominant (101) peak by means of well-known Scherrer's equation [31] which is 10.26 nm.
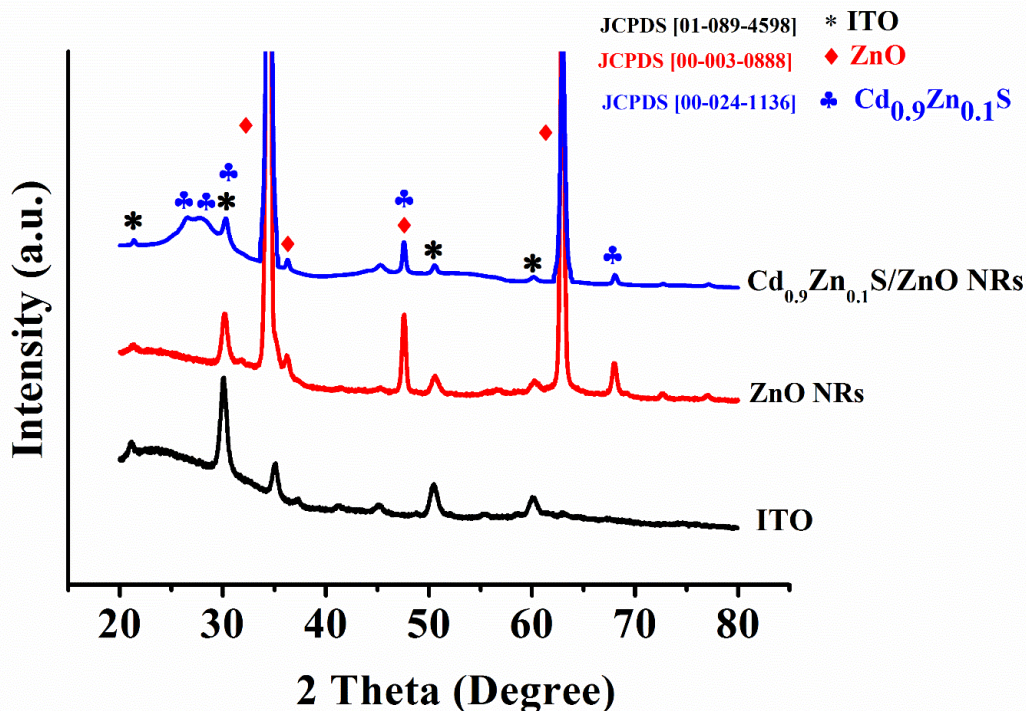

Figure 3. XRD spectra of nanostructured thin films: (a) ZnO NRs (b) $Cd_{0.9}Zn_{0.1}S$/ZnO NRs.

3.3 Surface Morphology and EDS Analysis

Figure 4(a-b) showed the top and cross-section views of FE-SEM images of pure ZnO NRs and the optimum sample $Cd_{0.9}Zn_{0.1}S$/ZnO NRs. Using the cross-section views, the thickness of the film of samples a and b was estimated to be about 500±10 nm and 600±30 nm, respectively. FESEM images demonstrate clearly that the morphology of both samples was obviously different. It can be seen distinguished by the diameter of rods (pure ZnO NRs and the optimum sample $Cd_{0.9}Zn_{0.1}S$/ZnO NRs) that are 70±10 nm, and 130±5 nm, respectively. This anomalous behaviour of samples was in accordance with the XRD results obtained for these samples.
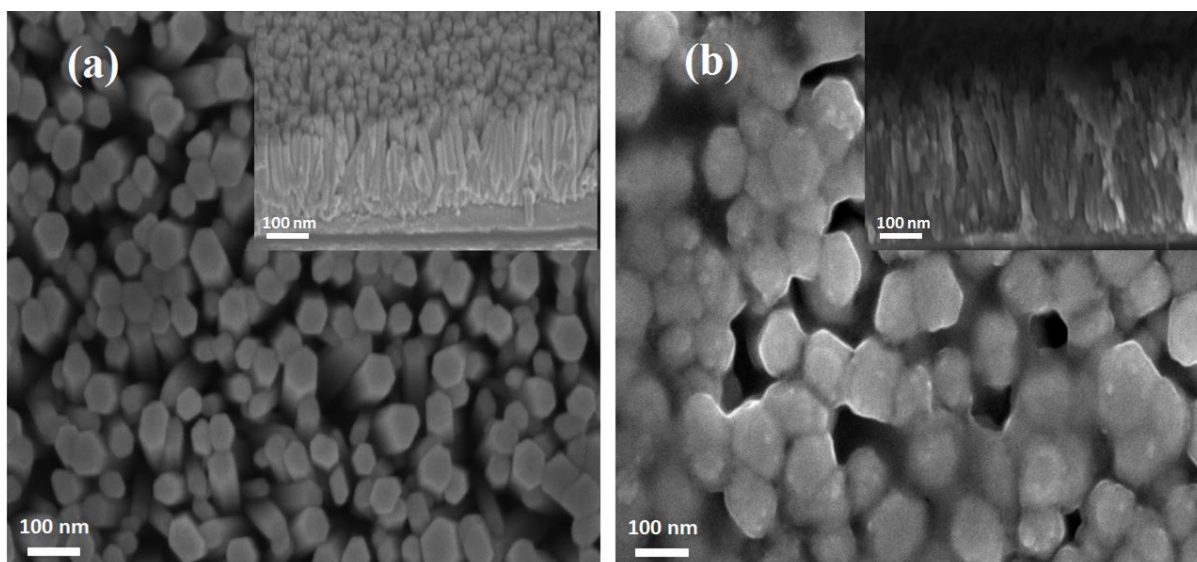
Figure 4. Top view and cross-sectional FE-SEM images of: (a) ZnO NRs(b) Cd0.9Zn0.1S/ZnO NRs.

EDX measurement for optimum sample $Cd_{0.9}Zn_{0.1}S$ is presented in Figure 5. The unidentified peaks correspond to the ITO substrate constituents. The average calculated composition of the precursor concentrations is 0.9 and the EDX measured value is close to 0.9. Therefore, the measured values of Cd and Zn are close to the calculated values. Consequently, the Cd and Zn reported values are similar to the estimated values. In addition, all elements' atomic ratio was measured and found during synthesis in near agreement with the ratio of the elemental chemical precursor solutions. This shows a stoichiometric composition of the sample.
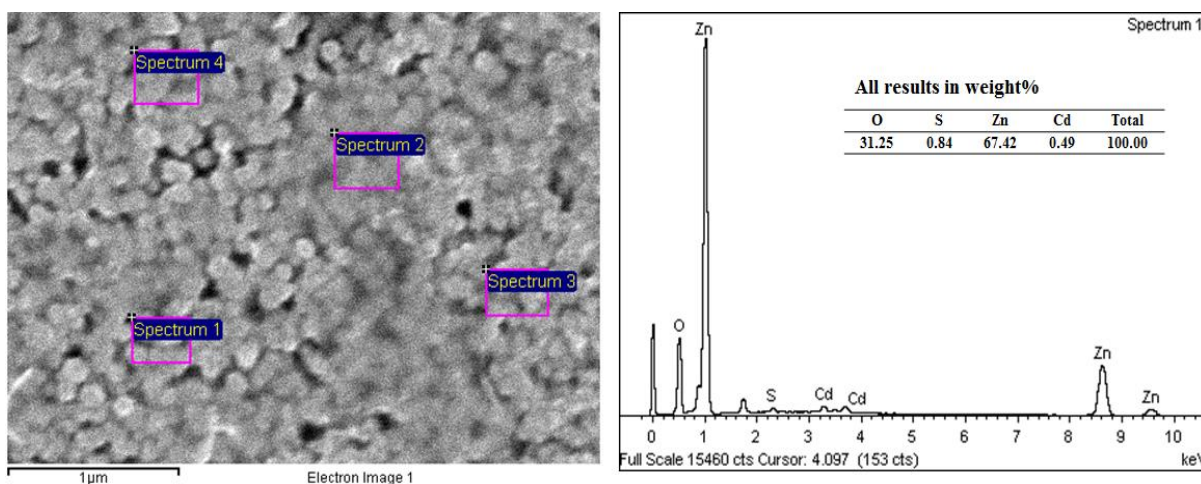

All results in weight%

O	S	Zn	Cd	Total
31.25	0.84	67.42	0.49	100.00

Figure 5. EDX spectrum of $Cd_{0.9}Zn_{0.1}S$/ZnO NRs.

3.4 Photoelectrochemical Performance

The PEC behaviours of different $Cd_xZn_{1-x}S$ electrodes were studied in 0.1 M Na_2S electrolyte under illumination. As shown in Figure 6, a very small photocurrent was observed for bra ZnO NRs and the photocurrent for different x of CdZnS substantially increased due to the integration of semiconductor nanomaterials. Moreover, the photocurrent response of the $Cd_{0.9}Zn_{0.1}S$/ZnO NRs nanocomposite was around nine times that of the pure ZnO NRs, this was ascribed by the fact that CdZnS can separate and store the photogenerated electrons, thus reducing the recombination rate of the photogenerated electrons and holes as well as enhancing the production of photocurrent [32].
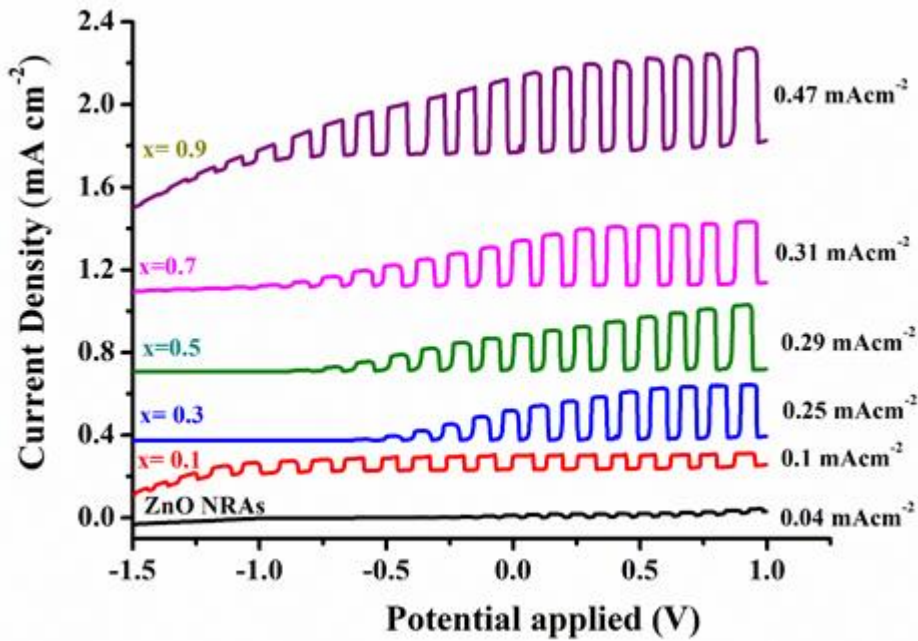
126

Figure 6. I–V curves of a- pure ZnO NRs; b- $Cd_xZn_{1-x}S$/ZnO NRs nanocomposites prepared at x.

Figure 7 shows that the cationic composition possessed a great influence on the photocurrent activities of $Cd_xZn_{1-x}S$/ZnO NRs nanocomposites. It is apparent that the photocurrent response of $Cd_xZn_{1-x}S$/ZnO NRs nanocomposites increases steadily with the x value ranging from 0.1 to 0.9. This is because the ternary compounds of $Cd_xZn_{1-x}S$ possess the property of regular variation in the bandgap energy by adjusting the content of x as shown in Figure 2. In order to use the solar spectrum efficiently, the main requirement is that the photoanode should have bandgap energy that closely matches the maximum light intensity in the visible spectrum. Hence, it can be easily developed to get a useful photoelectrochemical performance.
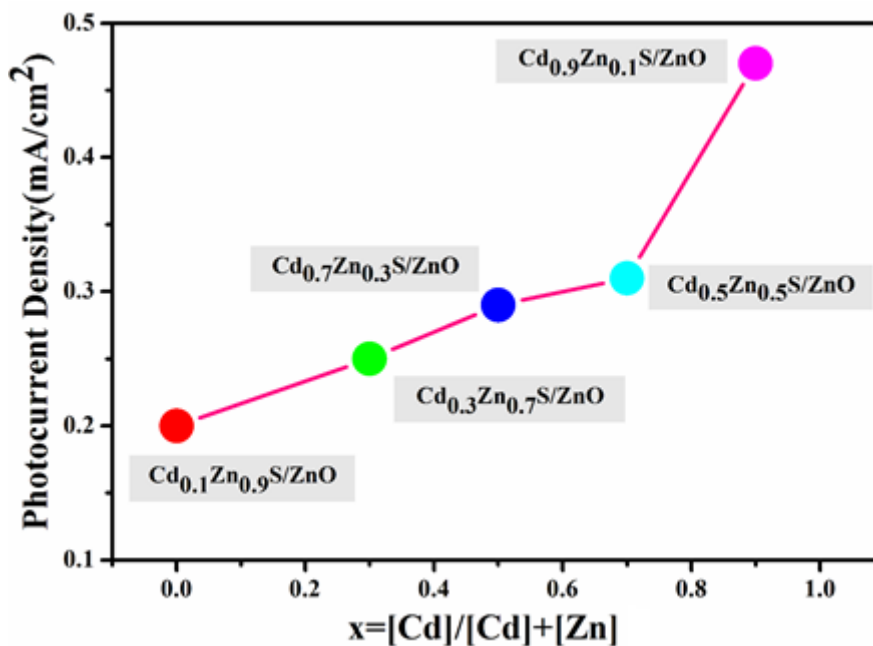

Figure 7. Photocurrent density values of $Cd_{0.9}Zn_{0.1}S$/ZnO NRs prepared at various x.

4. CONCLUSION

In conclusion, this study reports the synthesis and characterization of a group of nanocomposites $Cd_xZn_{1-x}S$ ternary semiconductor films covered ZnO NRs with different x values. They were prepared under ambient conditions through facile spin coating method. The XRD analysis, FE-SEM images and EDX analysis of the optimum sample $Cd_{0.9}Zn_{0.1}S$/ZnO NRs confirm the form of this ternary semiconductor. Furthermore, the energy gap shifted towards the low values when the x ratio is increased. The PEC activities of the $Cd_xZn_{1-x}S$/ZnO NRs nanocomposites were further investigated under illumination and the $Cd_{0.9}Zn_{0.1}S$/ZnO NRs nanocomposite was the most highly PEC active compared to the pristine ZnO NRs according to the findings of the present study. The PEC result shows that increasing Zn content leads to a decrease in photoresponse. Finally, it is found that the photoelectrochemical performance of these photoelectrodes increases with increasing the x ratio in composition $Cd_xZn_{1-x}S$. This noteworthy enhancement was attributed to increasing the molar ratio x made the $Cd_xZn_{1-x}S$/ZnO NRs more effective in the visible region which was confirmed via the energy gaps values

REFERENCES

[1] Lee, C.T., Materials **3**, 4 (2010) 2218-2259.
[2] Holi, A. M., Zainal, Z., Talib, Z. A., Lim, H. N., Yap, C. C., Chang, S. K. & Ayal, A. K., Optik. **127**, 23 (2016) 11111-11118.
[3] Liu, Y., Yufang, L., & Haibo, Z., J. Nanomaterials **2013** (2013).
[4] Ohtomo, A., Kawasaki, M., Sakurai, Y., Yoshida, Y., Koinuma, H., Yu P., Tang, Z. K., Wong, G. K., Segawa, Y., Mate. Sci. Eng. B. **54**, 1-2 (1998) 24-8.
[5] Pauporté, T. Synthesis of ZnO Nanostructures for Solar Cells- A Focus on Dye-Sensitized and Perovskite Solar Cells. In "The Future of Semiconductor Oxides in Next-Generation Solar Cells" Elsevier, Amsterdam. Chap. **1** (2017) 3-43.
[6] Zhu, L., Zeng, W., Sensors Actuat. A Phys. **1**, 267 (2017) 242-61.
[7] Holi, A. M., Zainal, Z., Talib, Z. A., Lim, H. N., Yap, C. C., Chang, S. K. & Ayal, A. K., Superlattice. Microst. **103** (2017) 295-303.
[8] Holi, A. M., Zainal, Z., Ayal, A. K., Chang, S. K., Lim, H. N., Talib, Z. A., Yap, C. C., Optik. **1**, 184 (2019) 473-479.
[9] Balachandran, S., Swaminathan, M., Dalton Trans. **42**, 15 (2013) 5338-47.
[10] Yamaguchi, T., Yamamoto, Y., Tanaka, Demizu, T. Y., & Yoshida, A., Thin solid films **281** (1996) 375-378
[11] Cardona, M., & Peter, Y. Y., Fundamentals of semiconductors. Springer-Verlag Berlin Heidelberg, (2005).
[12] Adachi, S. Handbook on physical properties of semiconductors. Springer Science & Business Media, (2004).
[13] Afzaal, M., & O'Brien P., J. Mate. Chem. **16**, 17 (2006) 1597-602.
[14] Abouelfotouh, F. A., Al Awadi, R., & Abd-Elnaby, M. M., Thin Solid Films **96**, 2 (1982) 169-73.
[15] Abid, H., Rekhila, G., Ait Ihaddadene, F., Bessekhouad, Y., & Trari, M., Inter. J. Hydrogen Energ. **44**, 21 (2019) 10301-10308.
[16] Kumar, P., Aparna M., Kumar, D., Neeraj D., Sharma, T. P., & Dixit, P. N., Opt. Mater. **27**, 2 (2004) 261-264.

[17] Rajathi, S., Sankarasubramanian, N., Ramanathan, K. & Senthamizhselvi, M., Chalcogenide Lett. **9**, 12 (2012) 495-500.

[18] Patidar, D., Saxena, N. S. & Sharma., T. P., J. Mod. Opt. **55**, 1 (2008) 79-88.

[19] Demir, R., & Gode. F., Chalcogenide Lett. **12**, 2 (2015) 43-50.

[20] Limei, Z. H. O. U., Yuzhi, X. U. E. & Jianfeng, L. I., J. Environ. Sci. **21** (2009) S76-S79.

[21] Zhu, G., Tian, L., Likun P., Zhuo S., & Changqing S., J. Alloys Comp. 5**09**, 2 (2011) 362-365.

[22] Dedova, T., Malle K., Volobujeva, O. & Oja, I., Phys. Status Solidi C **2**, 3 (2005) 1161-1166.

[23] Ray, S., Ratnabali B., & Barua, A. K., Jap. J. Appl. Phy. **19**, 10 (1980) 1889.

[24] Preisinger, A., & Pulker, H. K., Jap. J. Appl. Phy. **13**, S1 (1974) 769.

[25] Ramprakash, Y., Subramanian, V., Krishnakumar, R. Lakshmanan, A. S. & Venkatesan, V. K., J. power sources **24**, 1 (1988) 41-50.

[26] Kumar, V., Sharma, M. K., Gaur, J., & Sharma, T. P., Chalcogenide lett. **5**, 2 (2008) 289-295.

[27] Patidar, D., Sharma, R., Jain, N., Sharma, T. P. & Saxena, N. S., B. Mater. Sci. **29**, 1 (2006) 21-24.

[28] Yeo, S.-Y., Tae-Hyeong, K., Chang-Sun, P., Chang-Il, K., Ji-Sun, Y., Young-Hun, J., Youn-Woo, H., Jeong-Ho, C., & Jong-Hoo P., J. Electroceram. **41**, 1-4 (2018) 1-8.

[29] Tian, C. J., Rong, Z. T., Song, B. H., Wei L., Liang, H. F., Jing, Q. Z., & Li, L., Adv. Mater. Res. **225** (2011) 784-788.

[30] Mariappan, R., Ragavendar, M. & Ponnuswamy, V., J. Alloys Comp. **509**, 27 (2011) 7337-7343.

[31] Cullity, B. D., Elements of X-Ray Diffraction (Addision-Wesley, Reading, 1986) 78–103.

[32] Dongre, J. K., Mahim, C., Yuvraj, P., Sandhya, S., &. Jain, U. K., In AIP Conference Proceedings **1670**, 1(2015) 030007.